SEMARAK ILMU PUBLISHING

Journal of Advanced Research in Fluid Mechanics and Thermal Sciences

Journal homepage:
https://semarakilmu.com.my/journals/index.php/fluid_mechanics_thermal_sciences/index
ISSN: 2289-7879

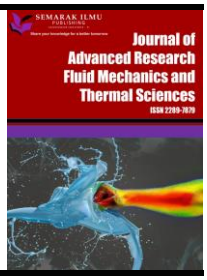

Numerical Analysis of Strut Thickness and Placement Effects on H-Darrieus Vertical-Axis Water Turbine

Yoyok Setyo Hadiwidodo[1,*], Radiktya Gilang Permana[2]

[1] Department of Ocean Engineering, Faculty of Marine Technology, Institut Teknologi Sepuluh Nopember (ITS) Surabaya, Indonesia
[2] Structural Integrity Research Center, Department of Ocean Engineering, Faculty of Marine Technology, Institut Teknologi Sepuluh Nopember (ITS) Surabaya, Indonesia

ARTICLE INFO

Article history:
Received 12 June 2024
Received in revised form 16 September 2024
Accepted 23 September 2024
Available online 10 October 2024

Keywords:
Vertical-axis water turbine; strut; computational fluid dynamics; finite element analysis

ABSTRACT

Vertical axis water turbines offer a promising technology for harnessing tidal currents to generate renewable electricity. However, these turbines are still under development and face challenges, particularly their susceptibility to fatigue due to vibrations, which can lead to failure. This study addresses the influence of radial forces on performance by analyzing the strut component of an H-Darrieus vertical axis water turbine. The analysis varies the strut's thickness and positioning using a one-way Fluid-Structure Interaction (FSI) approach. Three-dimensional models of different turbine configurations, including the flow domain, are created, and Computational Fluid Dynamics (CFD) simulations are performed to assess the turbine's torque. This torque data is then used in structural simulations via Finite Element Analysis (FEA) to evaluate the stress and deformation in various turbine models. The simulation results provide insights into optimal turbine designs under applied hydrodynamic loads.

1. Introduction

In the current era, fossil energy is gradually being abandoned, and many countries are transitioning to renewable energy. Indonesia, a nation rich in natural resources, has experienced a 7.3% average annual growth in electricity generation capacity between 2003 and 2013 [1]. Despite this progress, the adoption of renewable energy has been relatively slow, with renewables contributing only 6% to the national energy mix by 2021 [2]. This disparity is significant, especially considering Indonesia's targets outlined in the General National Energy Plan (RUEN), which aim to increase the share of New and Renewable Energy (NRE) to 23% by 2025 and 31% by 2050. These goals underscore the urgency of accelerating the integration of renewable energy into the country's energy infrastructure.

In this context, vertical-axis water turbines (VAWT) hold significant promise as a renewable energy source in Indonesia, given that 70% of the country's territory comprises water bodies. Despite their potential, these turbines are still in the research and field-testing stages before reaching

* *Corresponding author.*
E-mail address: ys.hadiwidodo@gmail.com

https://doi.org/10.37934/arfmts.122.1.163174

commercialization [3]. This is regrettable, given the numerous advantages of vertical-axis turbines over their horizontal-axis counterparts. The straightforward design of vertical-axis turbines, exemplified by the well-known H-Darrieus turbine, allows for a cost-effective manufacturing process [4]. Traditionally, the Darrieus turbine has been utilized as a wind turbine; however, its fundamental principles are similarly applicable to hydrofoil applications [5]. The concept of adapting Darrieus wind turbines for use as water turbines has garnered significant interest from researchers. In 1983, Miyake *et al.,* [6] conducted a theoretical hydrodynamic analysis of the Darrieus cross-flow water turbine using disk-blade element theory and vortex filament theory. This research was further developed with the establishment of an experimental setup, where experiments were carried out using a symmetrical NACA0012 blade profile to validate the theoretical findings from the previous year [7]. Vertical-axis turbines are not sensitive to flow direction, and their installation is uncomplicated since essential components like the drive train and generator remain on the water surface [8]. However, a notable weakness of this turbine type is the constant radial variation of fluid load on the turbine blades, which can lead to structural deformation fatigue and the potential for structural failure, commonly known as vibration [3,4].

According to Hara *et al.,* [9], the predominant focus in vertical-axis wind turbine research revolves around two-dimensional (2D) simulations due to their lower computational demand. Despite the increased accuracy offered by three-dimensional (3D) simulations compared to their 2D counterparts, the computational load for a 3D model is substantially higher, being at least 30 times that of a 2D model in turbine simulations [10]. Additionally, existing research tends to concentrate primarily on assessing the power performance of H-Darrieus turbines for wind and hydrokinetic applications, neglecting an in-depth examination of their structural integrity [8,11]. Sangi *et al.,* [11] highlighted the importance of considering the substantial difference in water density, which is 1000 times greater than that of air, in studies focusing on the structural integrity of Darrieus vertical axis turbines for water-based applications. In a separate study, Ali *et al.,* [8] employed numerical methods to analyze the structural behavior of H-Darrieus water turbines under various flow velocities and rotation rates, comparing their findings with experiments conducted by Huang *et al.,* [12]. The comparison revealed that the power estimates derived through CFD were higher than those obtained through experimental methods [8]. This underscores the understanding that numerical simulations depicting intricate flow patterns should be viewed as analytical and predictive tools, rather than flawless replicas of real-world behavior [13].

Several crucial parameters in turbine design include solidity, the number of blades, blade aspect ratio, and strut geometry [14]. Various studies have indicated that turbine blades typically experience low stress levels, with the highest stress concentrated in the turbine struts. Consequently, this study specifically addresses the impact of modifying struts on the structural integrity of the turbine. To enhance the precision of simulation results, this analysis incorporates hydrodynamic simulations conducted using 3D CFD methods. Following the hydrodynamic simulation results, separate structural simulations are carried out using FEA methods to assess the turbine's structural integrity. This approach is referred to as one-way FSI analysis, involving the transfer of fluid pressure data acting on the structure to the structural solver for subsequent analysis [15].

2. Methodology

2.1 Turbine Geometry

This study adopts the turbine dimensions and geometry outlined in a study conducted by Ali *et al.,* [8]. Detailed information on the turbine's geometry and dimensions is provided in Table 1 and Figure 1 and Figure 2. A three-dimensional geometric modeling of the turbine is conducted, which is

divided into three separate parts, namely three NACA0020 airfoil blades, strut, and the turbine's shaft, which are then assembled using CAD (Computer-Aided Design) based software. According to study conducted by Ali *et al.,* [8], the maximum stress on the turbine occurs on the strut-shaft connection, hence strut thickness is also increased from 6mm in original model to 10 mm in modified models. However, increasing strut thickness is accompanied by an increase in drag loss from the turbine and reduces turbine's aerodynamic performance [15,16]. Therefore, to reduce the elevated stress in that area, the positioning of the struts as supports and connections between the blades and the turbine shaft needs to be reassessed. Typically, turbine struts are symmetrically designed to align with the height position of the blades, ensuring a balanced rotor/shaft configuration [17].

Table 1
Turbine geometry parameters and dimensions

Geometry of the turbine	Dimensions
Blade pitch angles	0°
Blade height	1500 mm
Chord length	300 mm
Turbine diameter	1500 mm
Number of blades	3
Airfoil	NACA0020

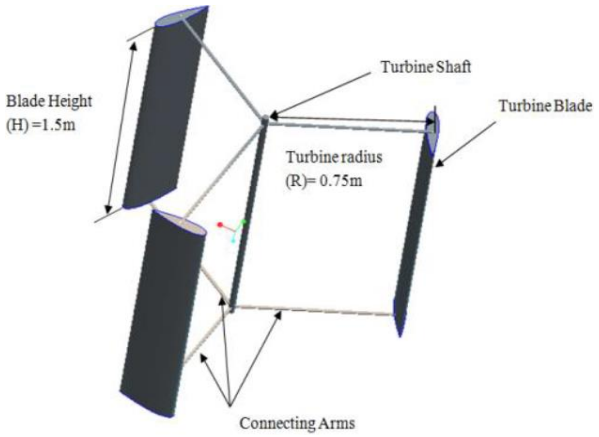

Fig. 1. Three-dimensional model illustration of the H-Darrieus turbine

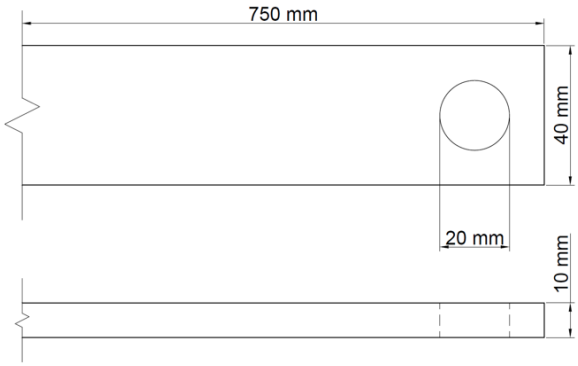

Fig. 2. Dimensions of the turbine strut

The turbine blades are made of aluminum alloy and modeled as solid components, while the struts and turbine shaft are modeled using structural steel. The material properties are detailed in Table 2.

Table 2
Material properties for aluminum and structural steel

Material properties	Aluminum	Structural steel
Density (kg/m^3)	2700	7850
Young modulus (GPa)	70	210
Poisson's ratio	0.33	0.30
Tensile yield strength (MPa)	276	250
Tensile ultimate strength (MPa)	310	460

This study investigates the analysis and modeling of H-Darrieus turbine struts, focusing on their spanwise connecting positions—specifically at the quarter span and the end span. The turbine, represented in 3D using CAD software, includes three variations of the H-Darrieus turbine model as

shown in Figure 3. To reduce deformation at the center of the blades, the second and third models adjust the strut positions toward the blade's middle, while the first model retains the design by Ali *et al.,* [8] as a reference for comparison.

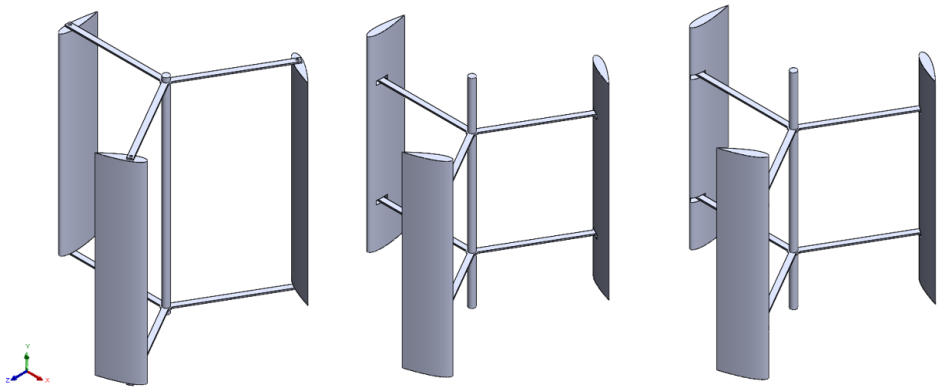

Fig. 3. H-Darrieus turbine 3D models

2.2 Fluid Domain Model

The fluid domain consists of a stationary domain and a rotary domain, with the dimensions of these domains determined based on the turbine diameter, as depicted in Figure 4. The rotating domain is represented as a 3D cylinder with a height of 2D, representing the rotational area of the turbine, while the stationary domain encompasses the outer part of the rotating domain.

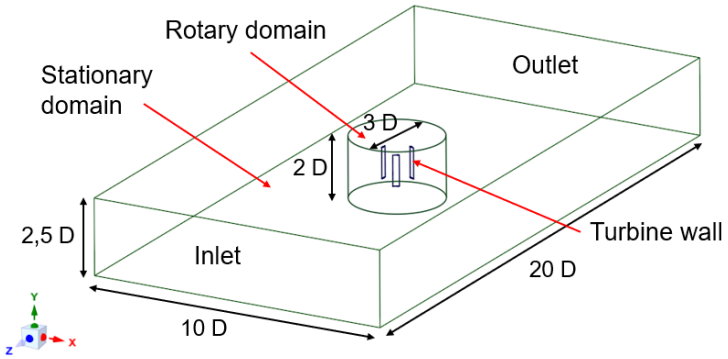

Fig. 4. Fluid flow domain model

2.3 Meshing

Due to the limitations of the computer's specifications, the number of mesh elements is reduced to decrease the simulation time. To simulate realistic conditions and calculate lift and drag forces on the turbine blade, mesh inflation was implemented around the turbine wall with a y+ value of 1 or less, focusing particularly on the surface of the turbine blade. The outcomes of meshing on the model of the fluid flow domain are presented in Table 3 and illustrated in Figure 5 to Figure 7. The meshing quality was evaluated, and the skewness value was found to be 0.856 (< 0.9), and the orthogonal quality value was 0.215 (> 0.2), indicating that it can be categorized as a good meshing, allowing for further simulations to be performed.

Table 3
Mesh analysis

Mesh Size	
General Mesh (mm)	300
Face Sizing Rotating Domain (mm)	75
Face Sizing Turbine (mm)	15
Inflation	
First layer thickness (mm)	1.9
Growth Rate	1.1
Number of Layers	10
Statistics	
Nodes	997616
Elements	5013879

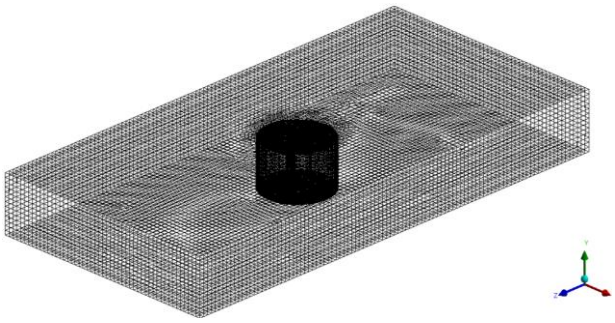

Fig. 5. Meshing at stationary domain

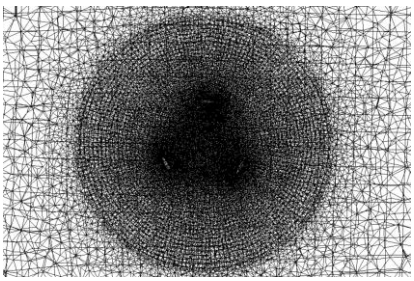

Fig. 6. Meshing at rotary domain

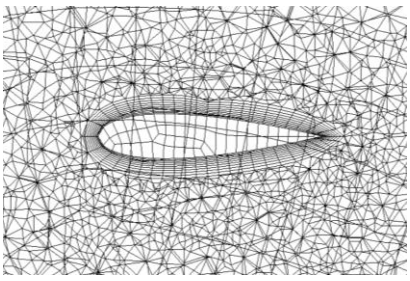

Fig. 7. Meshing at turbine blade

Figure 8 illustrates the meshing of the three turbine models, each using uniform element mesh sizes: 15 mm for the blades, 5 mm for the struts, and 10 mm for the turbine shaft. The third model has the highest element count, with 190,000 elements, due to its more complex strut-blade connection geometry. In comparison, model 2 has 180,000 elements, and model 1 has the fewest at 140,000 elements.

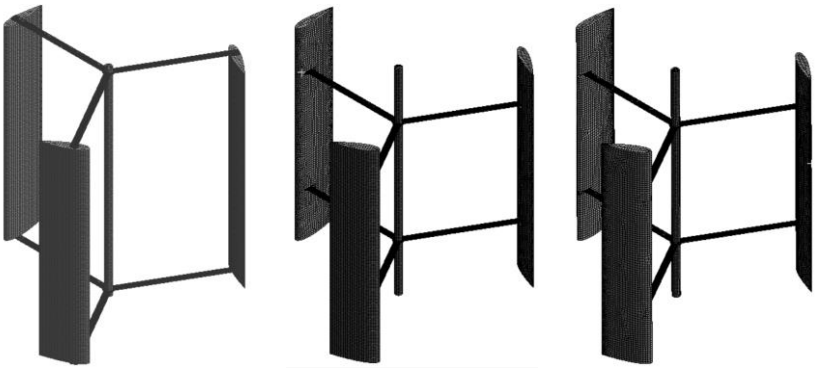

Fig. 8. Computational mesh for the turbine models; model 1, model 2, and model 3

2.4 Boundary Conditions

The specification of boundary conditions was conducted using numerical software, encompassing velocity inlet, turbine wall, and turbine rotational speed. Following the approach outlined by Ali *et al.,* [8], the freestream velocity of the flow ranges from 0.2 m/s to 1.4 m/s in alignment with the y-axis. To adopt a conservative approach, the highest freestream velocity, 1.4 m/s, is utilized, coupled with a turbine rotational speed of 5.86 rad/s. Under these conditions, the Tip Speed Ratio (TSR) of the turbine is determined as 3.14, employing the equation presented by Carriveau [18], as follows:

$$\text{TSR} = \gamma = \frac{\text{speed of rotor tip}}{\text{current free stream speed}} = \frac{v}{V} = \frac{\omega r}{V} \quad (1)$$

where the rotor tip speed (m/sec), v, current free stream speed (m/sec), V, rotor radius (m), r, angular velocity (rad/sec), ω and rotational frequency (Hz), f.

In Figure 9, several limitations or constraints of this structural analysis can be observed as follows:

(a) Annotation A represents the turbine rotational speed, which is 5.86 rad/s, perpendicular to the incoming flow direction or the y-axis.
(b) Annotation B indicates the surface that experiences the hydrodynamic loads.
(c) Annotation C represents the turbine shaft, defined as a fixed support, indicating that this part remains stationary and does not undergo deformation during the analysis.

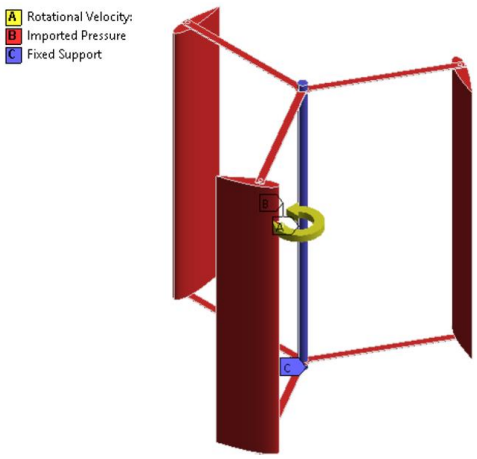

Fig. 9. Constrained and loads applied to the turbine model 1

3. Results

3.1 Hydrodynamics Simulation

In this segment, hydrodynamic simulation is carried out utilizing the 3D CFD method, facilitated by numerical software. The azimuth angle or rotational angle initiates at 0° and proceeds counterclockwise, as depicted in Figure 10. Here, V_0 represents the freestream velocity, VR denotes the resultant velocity for the blade at each azimuth position, and $V_\theta = R_\omega$, where ω is the angular velocity, and R is the turbine radius. The simulation procedure is executed for each 1° increment of the rotational angle, resulting in 360-time steps if the turbine completes one full rotation.

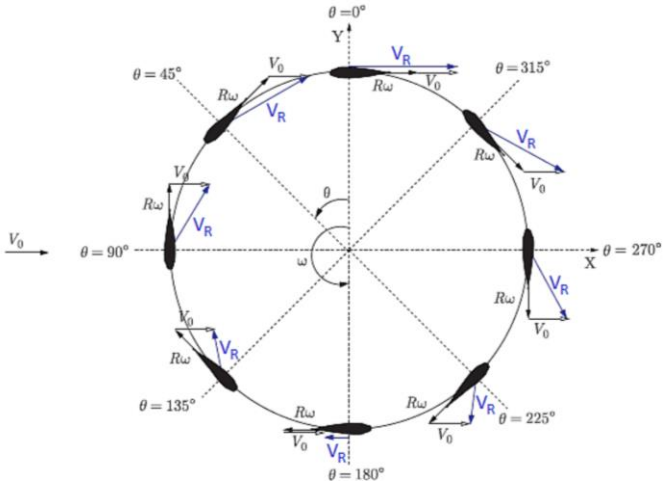

Fig. 10. Azimuth position and velocity triangle [19]

Referring to Satrio *et al.,* [20], the new turbine can provide a stable torque output starting from the fourth cycle with an angle increment between 1-5 degrees. For reliable outcomes, this research conducts simulations for 8 turbine cycles. The torque simulation outcomes for each turbine cycle are presented in Figure 11 and Table 4. Upon examination, the 1st to 3rd cycles displays fluctuations. The average moment generated becomes more consistent, notably from the 3rd to the 8th cycle, with an error margin of less than 5% compared to the preceding cycle.

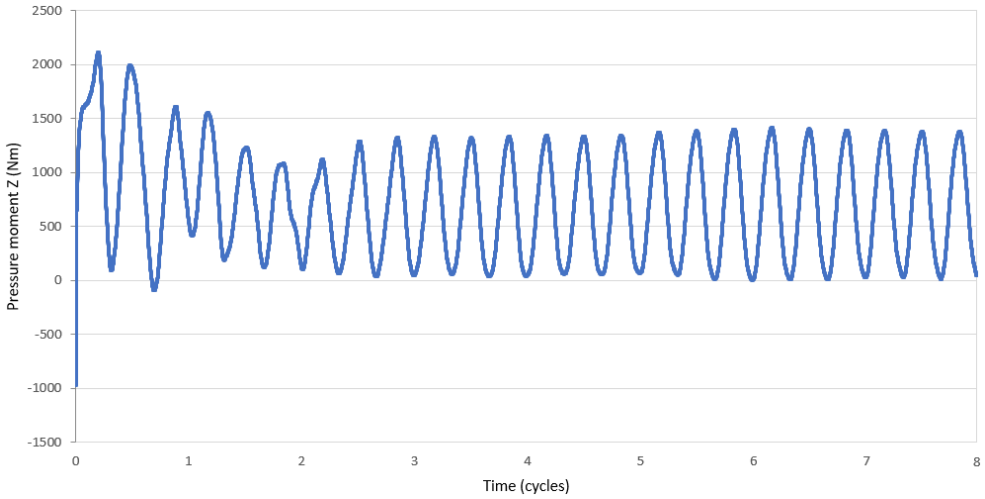

Fig. 11. Turbine pressure moment of each cycle

Table 4
Average moment of each turbine cycle

Turbine Cycle	1	2	3	4	5	6	7	8
Average Moment (Nm)	1119.83	752.79	623.16	642.71	651.03	671.38	680.96	692.76
Error from previous cycle (%)	-	-48.8	-20.8	3.0	1.3	3.0	1.4	1.7

Figure 12(a) and Figure 12(b) display the velocity and pressure contours for the turbine's third cycle at a 0° azimuth angle. With a freestream velocity of 1.4 m/s and a Tip Speed Ratio (TSR) of 3.14, the maximum velocity during the third cycle reaches approximately 6.2 m/s, concentrated around the turbine blade, as shown by the red contours. The fluid flow in the middle of the turbine opposes the freestream direction due to the influence of the returning blade's rotation. Additionally, high pressure is observed on the blade sections perpendicular to the freestream, marked by red contours, while low pressure is evident on the inner blade sections, indicated by blue contours. Figure 13(a) and Figure 13(b) reveal a significant pressure contrast at a 90° azimuth angle, with lower pressure inside the turbine compared to the outer sections, reflecting the pressure drop caused by the returning blade's rotation.

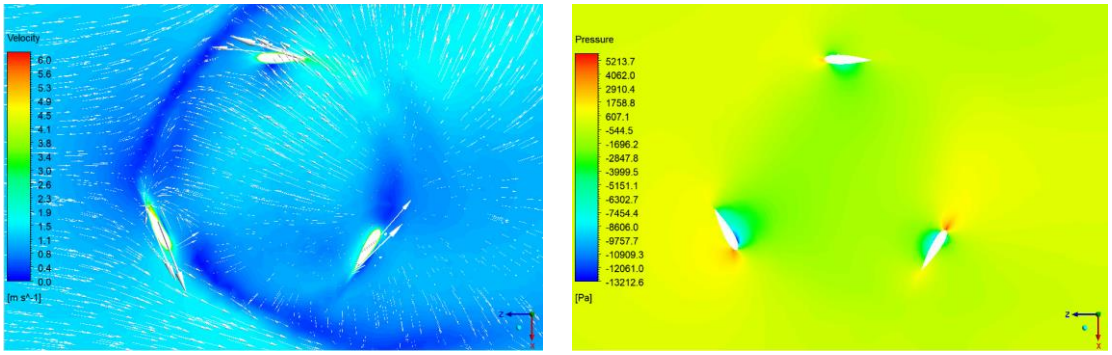

(a) (b)

Fig. 12. (a) Velocity contours and freestream direction, and (b) Pressure contour for the turbine's 3rd cycle at 0° azimuth angle

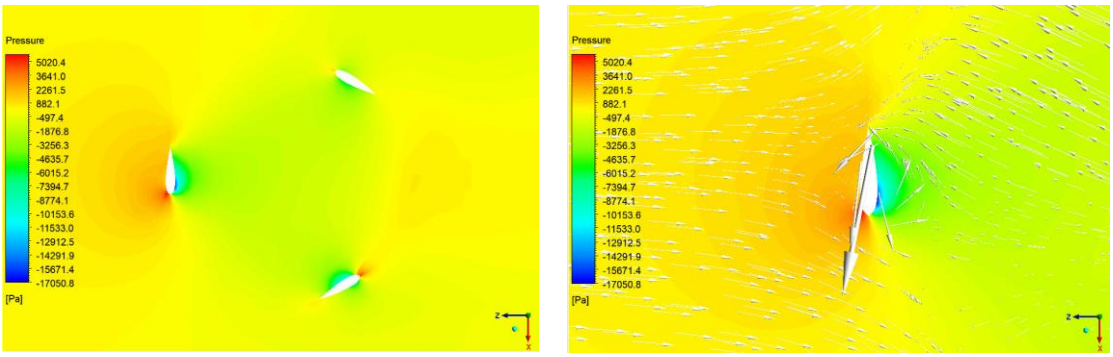

(a) (b)

Fig. 13. (a) Pressure contour for the turbine's 3rd cycle at 90° azimuth angle, (b) close up on the blade's outer sections

It is evident that an unstable flow or vortex exists at the end of the turbine blades in Figure 14, referred to as a tip vortex. This vortex continuously sheds during each blade revolution, leading to a reduction in torque and inducing structural vibrations. These vibrations result in torque loss and a decrease in efficiency [21].

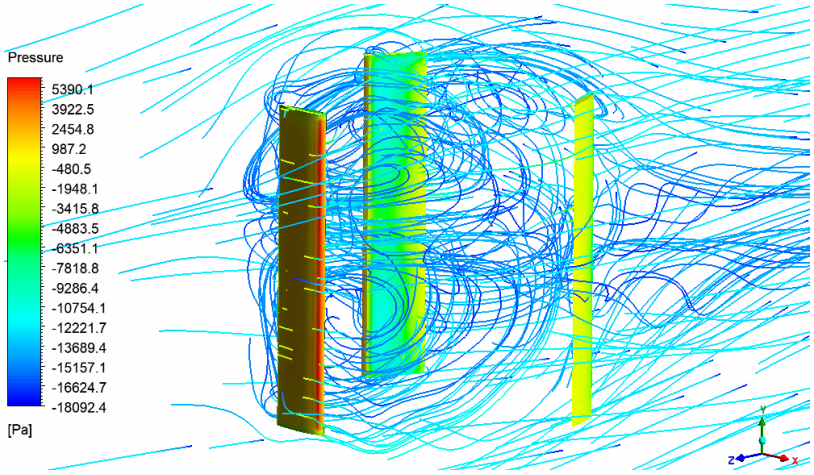

Fig. 14. Contours of pressure on the blade surface and streamlines around the turbine blade at a 90° azimuth angle

3.2 Structural Simulation

Following the hydrodynamic simulation, the fluid loads derived from the CFD analysis were imported into numerical software for additional structural analysis utilizing the Finite Element Analysis (FEA) method. This analysis aims to calculate the structure properties, such as stresses and deformation. The surface pressure distribution for all three turbine models is shown in Figure 15.

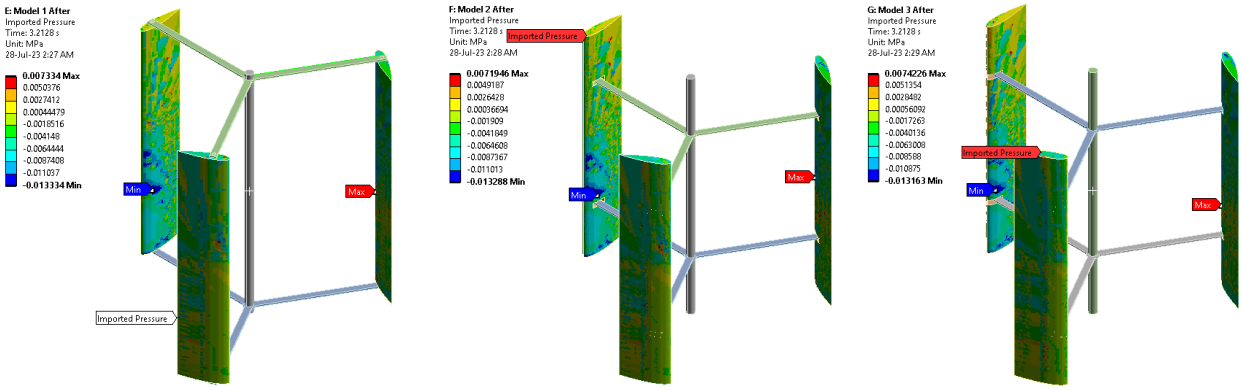

(a) Model 1 (b) Model 2 (c) Model 3

Fig. 15. Surface pressure distribution applied in turbine models

Figure 16 shows that the static simulation results indicate a reduction in maximum Von Mises stress and deformation in the turbine after modifying the strut. The highest stresses are concentrated at the connection between the turbine strut and the blade, while the lowest stresses occur on the turbine blades themselves, as illustrated in Figure 17. This highlights the importance of the strut-blade connection, where hydrodynamic forces from the water flow on the blades are transferred to the supporting structure. Additionally, the maximum deformation is observed on the turbine blades, particularly on the blade facing the flow, while the minimum deformation occurs near the turbine shaft, which serves as a fixed support. As shown in Figure 18, Turbine Model 1 exhibits the highest deformation, with a value of 0.87 mm at the center of the blade, whereas Turbine Model 2 has the lowest deformation, measuring 0.76 mm at the blade's edge.

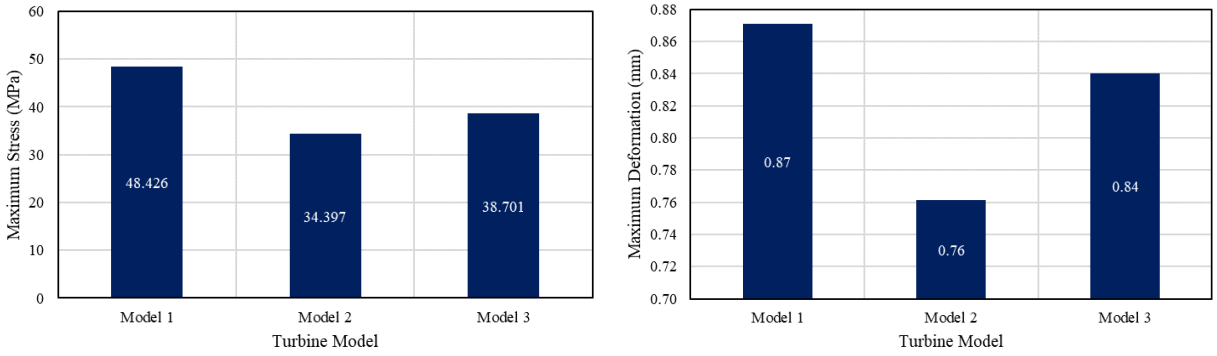

(a) (b)

Fig. 16. (a) Maximum Von Mises stress, and (b) maximum deformation on turbine models

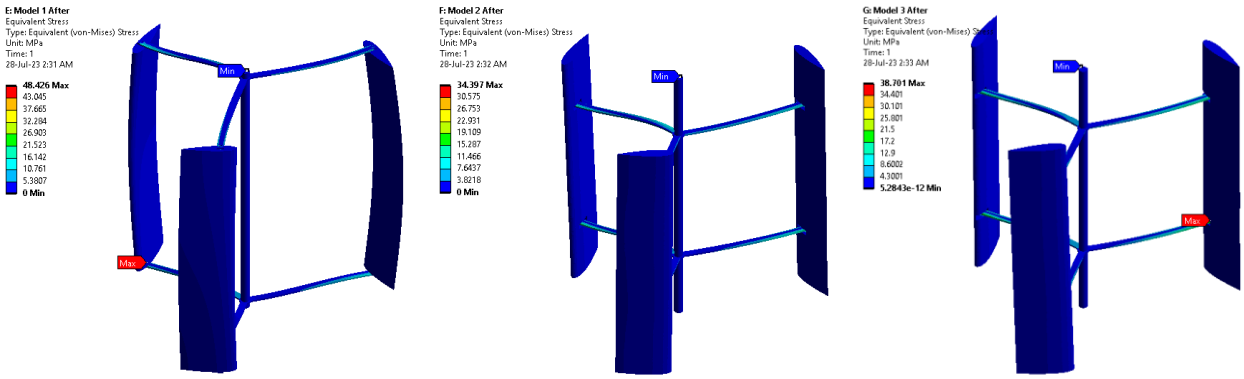

(a) Model 1 (b) Model 2 (c) Model 3

Fig. 17. Stress distribution of turbine models

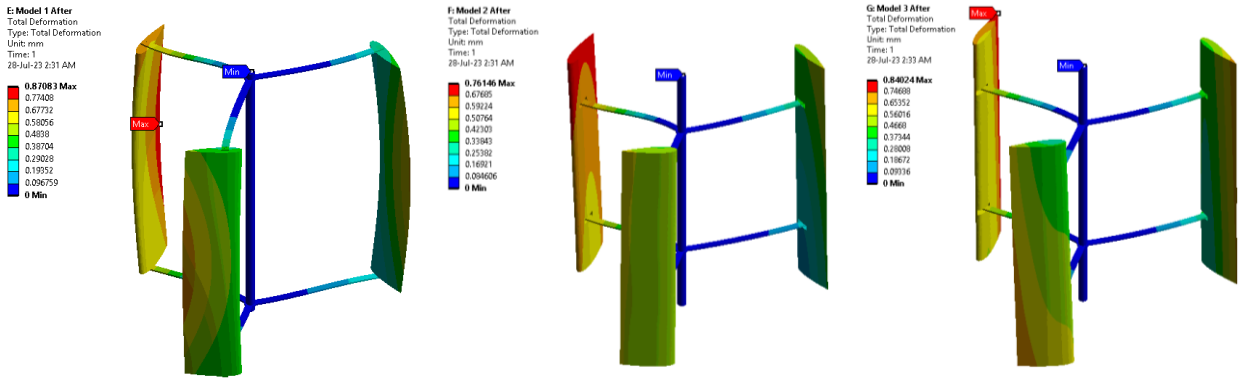

(a) Model 1 (b) Model 2 (c) Model 3

Fig. 18. Deformation distribution of turbine models

Moreover, the turbine fatigue life was determined using Soderberg theory. It is found that all the Turbine Models have fatigue life more than 1000000 cycles and safety factor value above 1. The safety factor distribution is shown in Figure 19 with Turbine Model 1 having the lowest safety factor with value of 1.78 and Turbine Model 2 has the highest safety factor with value of 2.506, both located in blade-strut connection.

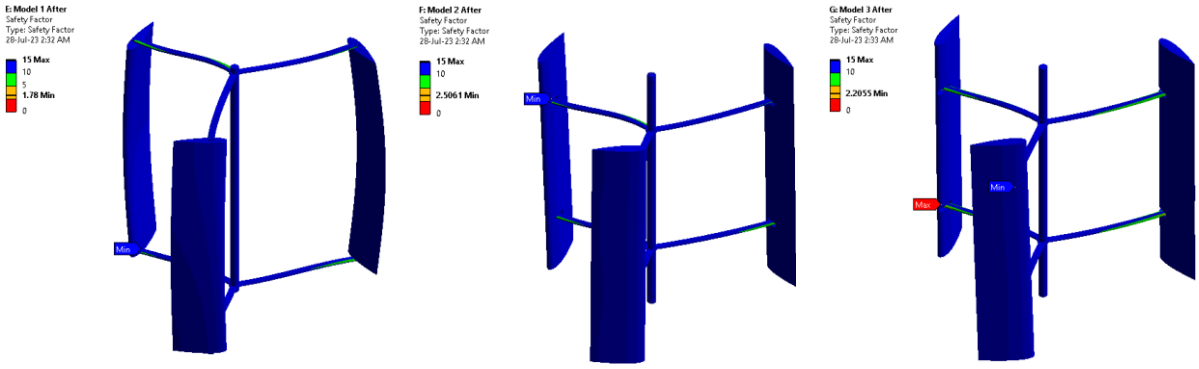

(a) Model 1 (b) Model 2 (c) Model 3

Fig. 19. Safety factor distribution of turbine models

4. Conclusions

In this study, the structural analysis of the vertical axis water turbine type H-Darrieus was conducted using a one-way FSI approach. To achieve realistic outcomes, a three-dimensional computational fluid dynamics (CFD) approach was employed for hydrodynamic simulation. The results of the hydrodynamic simulation indicate that with a free stream velocity of 1.4 m/s and a turbine rotational velocity of 5.68 rad/s, a TSR value of 3.14 was obtained. The torque moments occurring on the turbine became stable from the 3rd to the 8th revolution, with a percentage difference in average torque moments of less than 5%. This is in accordance with the theory presented by Satrio *et al.,* [20].

CFD simulation results were used to apply fluid loads to the turbine surface for further structural analysis using FEA. The analysis shows that the turbine model with modified struts generates lower stress and deformation compared to Turbine Model 1. Specifically, the H-Darrieus Turbine Model 2 exhibits the lowest Von Mises stress at 34.397 MPa—29% lower than Turbine Model 1 (48.426 MPa) and 11% lower than Turbine Model 3 (38.701 MPa). Additionally, Turbine Model 2 has the least deformation at 0.76 mm, which is 13% less than Turbine Model 1 (0.87 mm) and 9% less than Turbine Model 3 (0.84 mm).

Using Soderberg theory, the fatigue life of all three turbine models was determined to exceed 1,000,000 cycles, with safety factors above 1. Among the models, Turbine Model 1 had the lowest safety factor at 1.78, while Turbine Model 2 had the highest at 2.506, and Turbine Model 3 had a safety factor of 2.205. These results indicate that all three turbine models are structurally sound, as their maximum stress levels remain below their material yield strengths, and their safety factors are above 1. This suggests that the turbine strut is crucial in maintaining the structural integrity of the turbine. If the strut design is inadequate, cyclic fluid loads could induce fatigue, potentially leading to failure over time. Therefore, optimizing turbine design through material selection, proper geometry, and precise load distribution analysis is essential to enhance structural integrity and extend the turbine's operational lifespan.

Acknowledgement
This research was not funded by any grant. The authors express their deep appreciation to Allah, parents, mentors, and all individuals who offered invaluable aid and support, both in direct and indirect ways, during the progression of this research.

References

[1] Erinofiardi, Erinofiardi, Pritesh Gokhale, Abhijit Date, Aliakbar Akbarzadeh, Putra Bismantolo, Ahmad Fauzan Suryono, Afdhal Kurniawan Mainil, and Agus Nuramal. "A review on micro hydropower in Indonesia." *Energy Procedia* 110 (2017): 316-321. https://doi.org/10.1016/j.egypro.2017.03.146

[2] Adrian, Maisarah, Eko Priyo Purnomo, Ashley Enrici, and Tiara Khairunnisa. "Energy transition towards renewable energy in Indonesia." *Heritage and Sustainable Development* 5, no. 1 (2023): 107-118. https://doi.org/10.37868/hsd.v5i1.108

[3] Satrio, Dendy, I Ketut Aria Pria Utama, and Mukhtasor Mukhtasor. "Vertical axis tidal current turbine: Advantages and challenges review." *Proceeding of Ocean, Mechanical and Aerospace - Science and Engineering* 3 (2016): 64-71.

[4] Ali, Intizar, Shadi Khan Baloch, Saifullah Samo, and Tanweer Hussain. "Stress and fatigue life prediction of the H-type darrieus vertical axis turbine for micro-hydropower applications." *Journal of Mechanics of Continua and Mathematical Sciences* 16, no. 6 (2021): 28-38. https://doi.org/10.26782/jmcms.2021.06.00003

[5] Rehman, Wajiha, Fatima Rehman, and Muhammad Zain Malik. "A review of darrieus water turbines." In *ASME Power Conference*, vol. 51401, p. V002T12A015. American Society of Mechanical Engineers, 2018.

[6] Miyake, Yutaka, Tkuji Tsugawa, and Susumu Murata. "An Analysis of High-speed Type Cross flow Turbines." *Bulletin of JSME* 26, no. 211 (1983): 43-50. https://doi.org/10.1299/jsme1958.26.43

[7] Miyake, Yutaka, Keiichiroh Koike, Takuji Tsugawa, and Susumu Murata. "Performance characteristics of high speed-type cross flow turbine." *Bulletin of JSME* 27, no. 229 (1984): 1446-1453. https://doi.org/10.1299/jsme1958.27.1446

[8] Ali, Intizar, Shadi Khan Baloch, Saifullah Samo, and Tanweer Hussain. "Stress and fatigue life prediction of the H-type darrieus vertical axis turbine for micro-hydropower applications." *Journal of Mechanics of Continua and Mathematical Sciences* 16 (2021): 28-38. https://doi.org/10.26782/jmcms.2021.06.00003

[9] Hara, Yutaka, Naoki Horita, Shigeo Yoshida, Hiromichi Akimoto, and Takahiro Sumi. "Numerical analysis of effects of arms with different cross-sections on straight-bladed vertical axis wind turbine." *Energies* 12, no. 11 (2019): 2106. https://doi.org/10.3390/en12112106

[10] Li, Ye, and Sander M. Calisal. "Three-dimensional effects and arm effects on modeling a vertical axis tidal current turbine." *Renewable Energy* 35, no. 10 (2010): 2325-2334. https://doi.org/10.1016/j.renene.2010.03.002

[11] Sangi, Muhammad Jurial, Saifullah Samo, Shakil Ahmed Shaikh, Intizar Ali, and Tanweer Hussain. "One Way Fluid-structure Interaction Analysis of Vertical Axis Hydrokinetic Turbine." *International Journal on Emerging Technologies* 12, no. 1 (2021): 19-24.

[12] Huang, Sy-Ruen, Yen-Huai Ma, Chia-Fu Chen, Kazuichi Seki, and Toshiyuki Aso. "Theoretical and conditional monitoring of a small three-bladed vertical-axis micro-hydro turbine." *Energy Conversion and Management* 86 (2014): 727-734. https://doi.org/10.1016/j.enconman.2014.05.098

[13] Rezk, Kamal. "CFD as a Tool for Analysis of Complex Geometry." *Faculty of Technology and Science Environmental and Energy Systems, Karlstad University Studies*, 2010.

[14] Hand, Brian, and Andrew Cashman. "Conceptual design of a large-scale floating offshore vertical axis wind turbine." *Energy Procedia* 142, no. December (2017): 83-88. https://doi.org/10.1016/j.egypro.2017.12.014

[15] Wang, Zhi-Kui, Gwo-Chung Tsai, and Yi-Bao Chen. "One-way fluid-structure interaction simulation of an offshore wind turbine." *International Journal of Engineering and Technology Innovation* 4, no. 3 (2014): 127-137.

[16] Miao, Weipao, Qingsong Liu, Qiang Zhang, Zifei Xu, Chun Li, Minnan Yue, Wanfu Zhang, and Zhou Ye. "Recommendation for strut designs of vertical axis wind turbines: Effects of strut profiles and connecting configurations on the aerodynamic performance." *Energy Conversion and Management* 276 (2023): 116436. https://doi.org/10.1016/j.enconman.2022.116436

[17] Paraschivoiu, Ion. *Wind turbine design: with emphasis on Darrieus concept*. Presses inter Polytechnique, 2002.

[18] Carriveau, Rupp, ed. *Fundamental and advanced topics in wind power*. BoD-Books on Demand, 2011. https://doi.org/10.5772/731

[19] Hall, Taylor Jessica. *Numerical simulation of a cross flow marine hydrokinetic turbine*. University of Washington, 2012.

[20] Satrio, Dendy, I Ketut Aria Pria Utama, and Mukhtasor Mukhtasor. "Performance Enhancement Effort for Vertical-Axis Tidal-Current Turbine in Low Water Velocity." In *4th Asian Wave and Tidal Energy Conference (AWTEC)*. AWTEC, 2018.

[21] Jiang, Yichen, Chenlu He, Peidong Zhao, and Tiezhi Sun. "Investigation of blade tip shape for improving VAWT performance." *Journal of Marine Science and Engineering* 8, no. 3 (2020): 225. https://doi.org/10.3390/jmse8030225